Experiment of PI Controller for Indirect Current Control for Single – Phase Shunt Active Filter

Kanapot Yodmanee[1, *], Songklod Sriprang[1], Anurak Katwattanakul[2], Sakrit Noosawang[3] and Wanchak Lenwari[3]
[1] Department of Electrical Engineering Technology, Faculty of Industry and Technology, Rajamangala University of Technology Rattanakosin Wang Klai Kangwon Campus, Nongkea, Hua Hin, Prachuap Khiri Khan, 77110, Thailand
[2] Department of Electrical Engineering, Faculty of Engineering and Industrial Technology, Phetchaburi Rajabhat University Phetchaburi, Nawong, Muang, Phetchaburi, 76000, Thailand
[3] Department of Control System and Instrumentation Engineering, Faculty of Engineering, King Mongkut's University of Technology Thonburi, Bang Mod, Thung Khru, Bangkok, 10140, Thailand
***Corresponding Author E-mail:** Kanapot.yod@rmutr.ac.th
Received: Jun 13, 2024; **Revised:** Nov 06, 2024; **Accepted:** Nov 12, 2024

Abstract

Due to harmonic problems caused by various factors that resulted in damages and malfunctions of electrical equipment in the power system, eliminating harmonics in the electrical system has become an important issue for both industrial and household sectors. This article focuses on developing a current control method for a single-phase shunt active power filter (APF) that controls current by an indirect method. The detection of load current to generate reference signals uses the *dq*-axis reference frame for a single-phase electrical system. The design of circuit parameters and PI controller parameters for compensating current and DC bus voltage are based on a simple calculation method. Simulation and experimental results confirm that the proposed current control method and PI controller design effectively eliminate harmonics, with the percent of total current harmonic distortion (THDi) values of the supply current after compensation within the IEEE Std 519-2022 standard limit.

Keywords: Single–phase shunt active filter (SAF), Indirect current control, PI (Proportional-Integral), dq-axis, Harmonic Distortion

1. Introduction

The advent of electric vehicle (EV) technology, which has undergone significant advancements to replace internal combustion engine (ICE) vehicles, has prompted many companies in the automotive sector to quickly adapt. They are developing their own technologies to prepare for this transition. With the influence of leading electric vehicle technology companies like Tesla, especially with the advancements in efficient electric motor and battery technologies, vehicles can now travel longer distances. Therefore, battery charging equipment becomes crucial for electric vehicle systems, akin to a power source charging energy into the battery. However, the technology advancements also come with challenges, notably the battery charging equipment, which is a primary factor in rapidly charging or transferring electrical energy to the vehicle's battery with high electrical wattage. This results in high Total Harmonic Current Distortion (%THDi), which is harmful to the power supply system. Research on mitigating harmonic currents over a period of three years revealed that the impact of THDi resulted in damage and malfunctions of various electrical equipment in the power system, such as circuit breakers, due to the use of nonlinear loads like rectifiers, which convert alternating current to direct current, a fundamental circuit of battery chargers used in all types of electric vehicles, including personal electric vehicles, electric motorcycles, and electric golf carts. Consequently, these effects are unavoidable and can significantly affect the power system if left unaddressed. Therefore, a single-phase shunt active power filter circuit can effectively address this issue [1–4].

Detecting load currents to generate reference signals is the process of measuring any load current and performing mathematical calculations in various methods to derive the control system's reference signals. Several methods exist for detecting load currents to generate reference signals in active power filtering circuits, such as Fast Fourier Transform (FFT), Instantaneous reactive power theory, Kalman filter (KF), Neural network (NN), and Synchronous d-q reference frame [5]. However, in this article, the researchers chose to use the method of detecting load currents to generate reference signals in the D-Q Reference Frame using the basics of Park Transformation. To apply this method in a single-phase electrical system, it is placed on the stationary reference frame by introducing imaginary variables so

that the values of the variables or signals assumed are shifted back 90 degrees or -π/2 [6].

From related research studies on current control of shunt active filters, two primary methods can be distinguished: direct current control and indirect current control. In direct current control, harmonic current is used as the reference signal to control the compensating current to match the reference signal, effectively eliminating harmonic currents in the electrical system and making the source current closely resemble a sinusoidal waveform at the fundamental frequency [7–9]. However, designing controllers in this manner presents challenges in tracking the reference signal due to its harmonic nature, which involves multiple frequencies. The control design must consider the bandwidth of the highest-order harmonics, known to be beyond the suitable range for a PI controller, which is not ideal for controlling signals with high bandwidths. Conversely, indirect current control uses a sinusoidal reference signal at the fundamental frequency to command the source current to match the reference current. This control method is suitable for a PI controller, as the required bandwidth of the signal is low, equivalent to the fundamental frequency, making the control design straightforward. Several researchers have proposed indirect current control methods [10–11] and found this control approach to be satisfactory, capable of reducing the number of sensors required for measurement.

This article presents the design and implementation of a PI controller for a single-phase shunt active filter based on the indirect current control technique. Simulation results and actual testing demonstrate the effectiveness of eliminating harmonic currents in the electrical system, aligning with the IEEE Std 519-2022 standard.

2. Single-Phase Shunt Active Filter

2.1 The fundamental principle

The Single-Phase Shunt Active Filter circuit functions as a filter to reduce or eliminate harmonic currents from the electrical system, ensuring that the supply current closely resembles a sinusoidal waveform or matches the supply frequency. As depicted in **Figure 1**, the structure of the Single-Phase Shunt Active Filter circuit comprises essential components including the supply utility, nonlinear load, and inverter circuit, which acts as a current source when operating with a controlled rectifier. The components of the Single-Phase Shunt Active Filter inverter circuit consist of four IGBTs (Insulated Gate Bipolar Transistors), four power diodes, one capacitor and one shunt active inductor. The operating principle of the Single-Phase Shunt Active Filter circuit begins with measuring the load current entering the control system to calculate and determine the required compensation current reference. Once the control current reference is obtained, the control system calculates appropriate values to switch the four IGBTs of the inverter.

The inverter acts as a voltage source with a capacitor connected in parallel with the IGBTs, as shown in **Figure 1,** serving as the energy source for supplying voltage to the inverter. When the output voltage of the inverter exceeds the supply system voltage appropriately, it creates a voltage drop across the inductor, resulting in current flowing through the inductor to the supply current, thus generating compensation current. This injected compensation current is the difference between the supply current and the load current. When the compensation current is injected, it causes the supply system current to closely resemble a sinusoidal waveform, eliminating harmonics and leaving only the fundamental frequency. However, the control system design needs to be in a closed-loop form to ensure the system's controllability and stability.

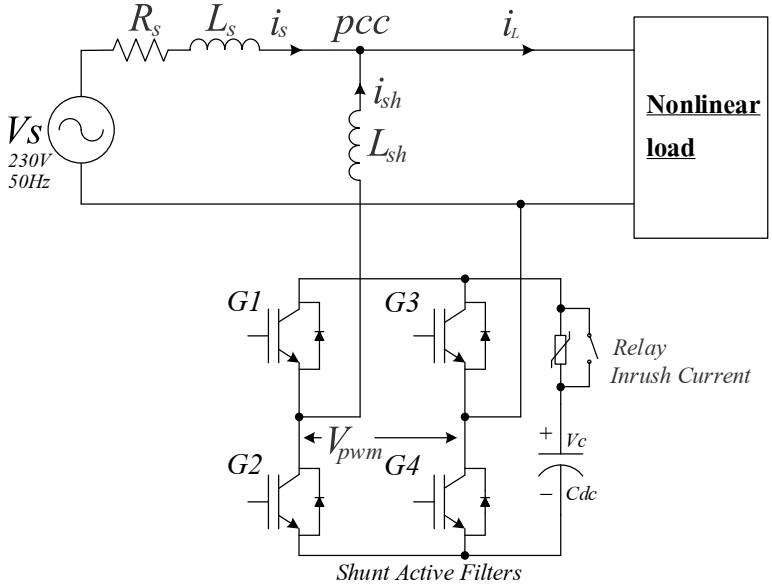

Figure 1 The conventional scheme of a Single-Phase Shunt Active Filter

2.2 Direct Current Control

Direct current control, as shown in **Figure 2**, the reference signal (i_{sh}^{*}) is the harmonic current calculated from the load current (i_L) and the current passing through the inductor (i_{sh}). This signal is feedback into the control system to ensure the system can inject compensation current according to the reference signal. This process eliminates harmonic currents in the electrical system, making the supply current resemble a sinusoidal waveform, leaving only the fundamental frequency [12–14]. However, in this control method, the reference signal (i_{sh}^{*}) contains harmonic components of various frequencies, which means the controller design must consider the bandwidth of the highest-order harmonics to achieve effective control. Therefore, it is necessary to select a controller type suitable for handling high-bandwidth currents, such as Fuzzy Logic control [12], Robust control [15], Dead-beat control [16], and PR (Proportional + Resonant) [17]. Nevertheless, direct current control methods for shunt active filters still often employ PI (Proportional-Integral) and PID (Proportional-Integral-Derivative) current controllers.

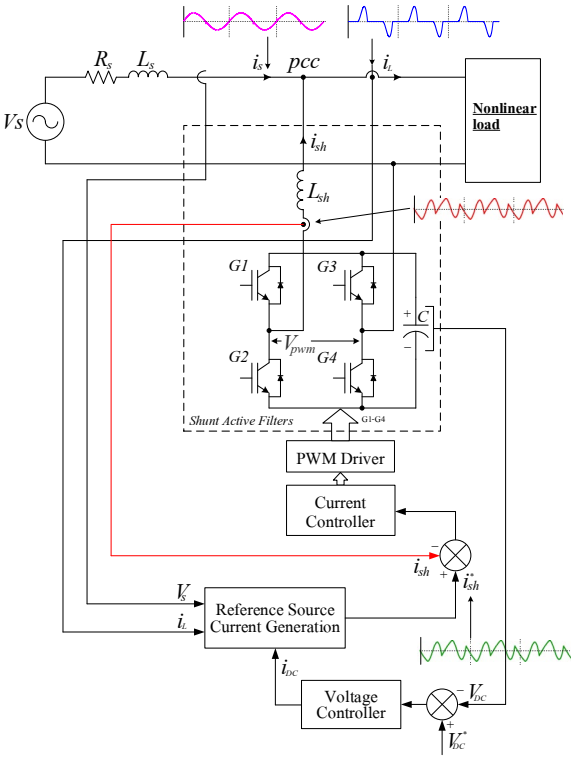

Figure 2 The structure of a single-phase shunt active filter with direct current control.

2.3 Indirect Current Control

The indirect current control of the single-phase shunt active filter, as shown in **Figure 3**, uses a reference signal (i_s^{*}) that is a sinusoidal current waveform with a frequency equal to the fundamental frequency. This reference signal is calculated from measuring the load current (i_L) and the supply current (i_s) to provide feedback to the control system. The aim is to force the supply current to be a sinusoidal waveform with a frequency matching the fundamental frequency according to the reference signal, thereby eliminating harmonic currents regardless of the waveform of the current passing through the inductor (i_{sh}) [18–21]. Consequently, the researcher has chosen to use the indirect current control method for the single-phase shunt active filter. This method's advantage is that the reference signal (i_s^{*}) is a sinusoidal waveform with a frequency equal to the fundamental frequency, which is 50 Hz, resulting in a low bandwidth. This allows for the use of less complex controllers, such as Hysteresis control and PI controllers, which are suitable for controlling signals with low bandwidth and simplifying the design of controller parameters.

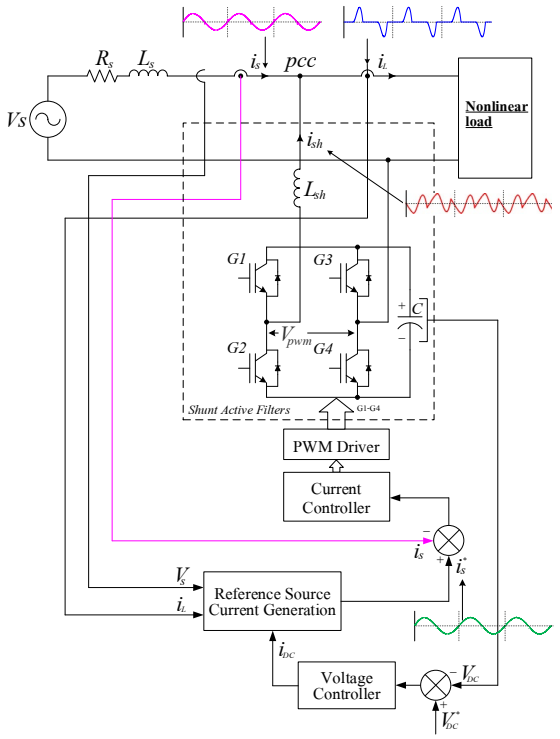

Figure 3 The structure of a single-phase shunt active filter with indirect current control.

3. Proposed Control Scheme

It is well known that converting electrical energy from alternating current (AC) to direct current (DC) using a rectifier circuit to supply power to a load, known as a nonlinear load, results in harmonic currents at the supply. These harmonics distort the waveform from its sinusoidal shape due to the presence of additional frequencies in the system. The design principle and method proposed, as illustrated in **Figure 4**, start by determining the reference current (i_s^{*}) by measuring the load current (i_L) and the supply voltage (V_s). These measurements are input into the Harmonic Current Extraction block, using the d-q Transformation principle to determine the amplitude of the load current at the fundamental frequency of 50 Hz ($\bar{i}_{Ld}$). Another crucial aspect of the active filter's operation is maintaining the DC bus voltage. The outer loop control

maintains the voltage at 450 volts using a PI controller, which serves as the energy source for the inverter to generate compensating current through the active inductor (L_{sh}). The output from the PI Voltage Controller, i_{DC}, is added to $\bar{\imath}_{Ld}$ to obtain the reference current i_S^*. The inner loop control, which manages the compensating current, also uses a PI controller. Due to the selection of indirect current control for the active filter, this approach results in a low bandwidth, allowing the use of a less complex and effective controller. Nonetheless, designing the PI controller to find the Controller Gains for both loops is done using a specified method, selecting appropriate values for governing damping and natural frequency.

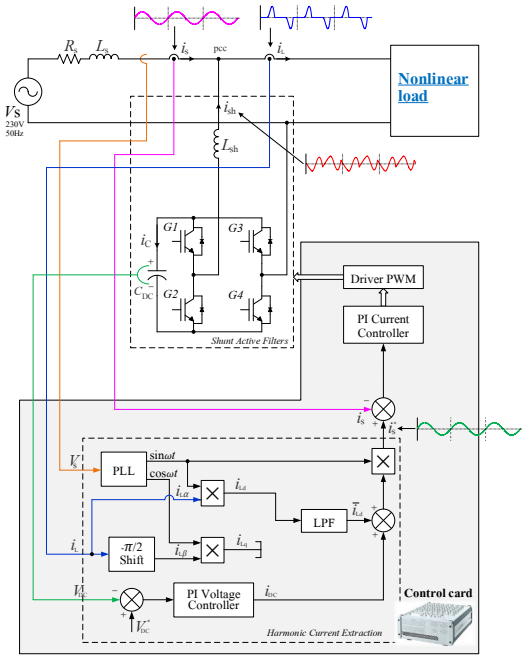

Figure 4 The proposed control scheme

3.1 Reference Current Generation Techniques

The detection of the load current to determine the reference current signal (i_S^*) utilizes the fundamental method of the Park Transformation [22]. The load current (i_L) is transformed to the stationary reference frame ($\alpha - \beta$), resulting in the variables $i_{L\alpha}$ and $i_{L\beta}$. The $i_{L\beta}$ is obtained by shifting the load current (i_L) by -90 degrees or -π/2. Next, these variables are transformed to the rotating reference frame (D-Q Reference frame) using the phase angle (θ) or ωt derived from the PLL (Phase-Locked Loop) block, which in turn is obtained from the measurement of the supply voltage. The result of this transformation is i_{Ld} and i_{Lq}, with i_{Lq} not used. The i_{Ld} signal is then passed through a Low Pass Filter set at 10 Hz to obtain a DC-like signal $\bar{\imath}_{Ld}$, which is added to the result from the DC bus controller i_{DC}. Finally, the signal is transformed back to the stationary reference frame. Therefore, the result is the reference current signal i_S^*, as shown in Eq. (1).

$$i_S^*(\omega t) = (\bar{\imath}_{Ld} + i_{DC})\, sin\, \omega\, t \qquad (1)$$

3.2 Controller Design

Considering **Figure 4**, the single-phase shunt active filter is connected to the utility grid, functioning to compensate for the distorted current waveform caused by the load connected at the PCC (Point of Common Coupling). If the utility grid is assumed to be an infinite load, the equivalent circuit of the inner current control loop is shown in **Figure 5**. Power is transferred through the inductor (L_{sh}) by controlling the duty cycle of the single-phase shunt active filter, which is the output derived from the DC voltage control circuit across the capacitor (C_{DC}). As shown in the **Figure 5**, this represents the equivalent circuit of the single-phase shunt active filter. The open-loop transfer function of the inner current control loop can be derived as shown in Eq. (2). However, due to the very low resistance in the inductor, it is omitted, as shown in Eq. (3). Then, by applying the Laplace transform to Eq. (3), Eq. (4) is obtained.

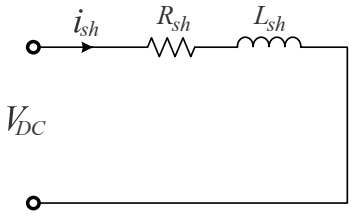

Figure 5 Equivalent circuit of a single-phase shunt active power filter

$$V_{DC} = R_{sh} i_{sh} + L_{sh} \frac{di_{sh}}{dt} \qquad (2)$$

$$V_{DC} = L_{sh} \frac{di_{sh}}{dt} \qquad (3)$$

$$V_{DC}(s) = sL_{sh} I_{sh}(s) \qquad (4)$$

From Eq. (4), the open-loop transfer function of the inner current control loop can be obtained as shown in Eq. (5).

$$\frac{I_{sh}(s)}{V_{DC}(s)} = \frac{1}{sL_{sh}} \qquad (5)$$

However, considering **Figure 4**, the capacitor at the DC bus (C_{DC}) is charged and discharged by the single-phase shunt active filter circuit. The differential equation can be written as shown in Eq. (6). Then, applying the Laplace transform yields Eq. (7).

$$i_C = C_{DC} \frac{dV_{DC}}{dt} \qquad (6)$$

$$I_C(s) = sC_{DC} V_{DC}(s) \qquad (7)$$

From Eq. (7), the open-loop transfer function of the outer voltage control loop at the DC bus can be obtained as shown in Eq. (8).

$$\frac{V_{DC}(s)}{I_C(s)} = \frac{1}{sC_{DC}} \qquad (8)$$

The control of compensating current using PI controllers is an effective and easily designable method. To control compensating current using PI controllers, it is necessary to work in conjunction with Pulse Width Modulation (PWM) switching techniques to generate control pulses for the IGBT switch devices in the shunt active filter circuit, as shown in **Figure 4**. The block diagram represented the PI controller design can be seen in **Figures 6–7**. From the diagram, the difference between the reference current (i_s^*) obtained through harmonic detection using the single-phase d-q transformation method and the supply current (i_s) injected by the active filter circuit is fed as an input to the PI controller. The output is then set as the reference voltage (U^*) to be passed through the plant, represented by the shunt inductor (L_{sh}), to simulate the compensating current (i_{sh}) on the output side. This compensating current (i_{sh}) is therefore related to the result of the difference between i_s^* and i_s.

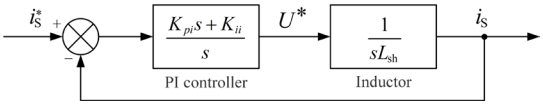

Figure 6 Block diagram of the compensating current control system

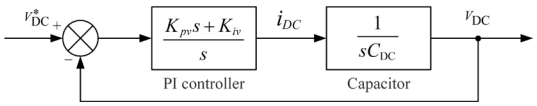

Figure 7 Block diagram of the DC-bus Voltage control system

From the block diagram of the control system, the closed-loop transfer functions can be derived. Eq. (9) represents the transfer function for the current loop, while Eq. (10) represents the transfer function for the voltage loop. The design of the PI controller involves an approximation method by comparing the performance of the control system transfer function with the standard second-order transfer function, as stated in Eq. (11). This comparison leads to the Eqs. (12)–(15), which allow for the design of the K_{pi}, K_{ii} values for the current loop, and K_{pv}, K_{iv} values for the DC-bus voltage loop, respectively [23].

$$\frac{i_S}{i_S^*} = \frac{\left(\frac{K_{pi}s+K_{ii}}{L_{sh}}\right)}{s^2+\left(\frac{K_{pi}}{L_{sh}}\right)s+\frac{K_{ii}}{L_{sh}}} \quad (9)$$

$$\frac{V_{DC}}{V_{DC}^*} = \frac{\left(\frac{K_{pv}s+K_{iv}}{C_{DC}}\right)}{s^2+\left(\frac{K_{pv}}{C_{DC}}\right)s+\frac{K_{iv}}{C_{DC}}} \quad (10)$$

$$T(s) = \frac{\omega_n^2}{s^2+2\zeta s\omega_n+\omega_n^2} \quad (11)$$

$$K_{pi} = 2\zeta_1\omega_{n1}L_{sh} \quad (12)$$

$$K_{ii} = \omega_{n1}^2 L_{sh} \quad (13)$$

$$K_{pv} = 2\zeta_2\omega_{n2}C_{DC} \quad (14)$$

$$K_{iv} = \omega_{n2}^2 C_{DC} \quad (15)$$

A properly designed compensator is required for a stable closed-loop Single-phase SAF with appropriate performance. The typical procedure of compensator design is as follows: 1) Collect system parameters such as input voltage, output voltage, maximum load/output current, switching frequency, input and output capacitance, and output inductance. 2) Determine the transfer function of the system. 3) Determine the zero-crossover frequency of the inner loop, i.e., the current loop first. Usually, this frequency is chosen at least equal to 1/10 to 1/5 of the switching frequency. As shown in **Figure 8**, the switching frequency is ω_s, and the zero-crossover frequency is $\omega_{n1} = (1/351)\omega_s$. 4) Determine the compensation type. The compensation type is determined by the location of zero crossover frequency and the characteristics of the proposed system.
5) Determine the desired location of the poles and zeros of the selected compensator. By following the mentioned procedure, the controller design of the Single-phase SAF making sure the system is stable and attenuation of switching noise, is expressed as follows.

The zero-crossover frequency settings of the designed current and voltage control laws are presented in **Figure 8**. The switching frequency (f_s) of the shunt active filter is set to 25 kHz (ω_s = 157,079 rad/s). The current loop, which is the inner loop, is designed to have a higher bandwidth compared to the outer DC-bus voltage loop. According to the Nyquist-Shannon theory [24], the natural frequency (ω_{n1}) for the current loop should be chosen to be less than half of the switching frequency (ω_s). Thus, a value of approximately 1000 rad/s is selected for ω_{n1}. For the DC-bus voltage loop, the natural frequency (ω_{n2}) is set to 20 rad/s, which is 50 times lower than ω_{n1}. These values are depicted in **Figure 8**, enabling the determination of the stability boundaries for the overall system. The unstable region lies beyond the natural frequency ω_{n1}. To ensure transient behaviors with low overshoot and fast response, the damping ratios ζ_1 and ζ_2 are tuned to be 0.05 and 0.25, respectively. However, for the presented work, the values ω_{n1} = 447.39 rad/s and ω_{n2} = 22.36 rad/s have been determined, which resulted in the best response obtained from the experiments. This success can be attributed to the use of the defining and selecting method for governing damping and natural frequency.

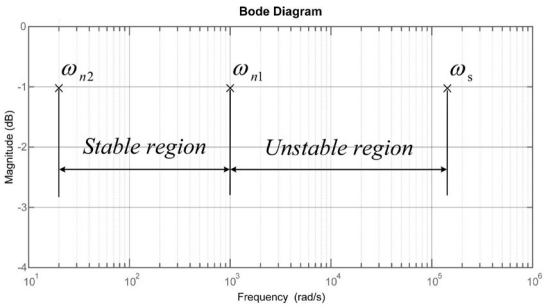

Figure 8 The zero-crossover frequency settings of the designed controllers

4. Simulation and Experimental Validation

4.1 Simulation Results

The following simulation results confirm the proposed concept outlined above. The simulations were conducted using MATLAB/SIMULINK, with the sampling time set to align with realistic values for both the power and control sections. The control section's sampling time was set to $1/f_s$, while the power section's sampling time was set to 100 times that of the control section. The parameters and components of the active filter used in the simulations and actual experiments are shown in **Table 1**. **Figures 9–10** show the results of measuring the load current (i_L) to generate the reference current signal (i_s^*), which follows the theory discussed in section 3.1. The resulting signal retains only the fundamental frequency load current at 50 Hz without harmonic distortion. Additionally, the Bus DC voltage is effectively maintained at 450 volts.

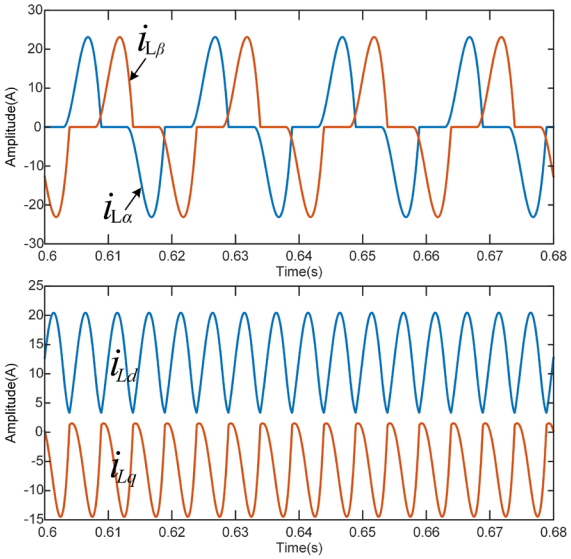

Figure 9 $i_{L\alpha}$, $i_{L\beta}$, i_{Ld} and i_{Lq}: After compensation

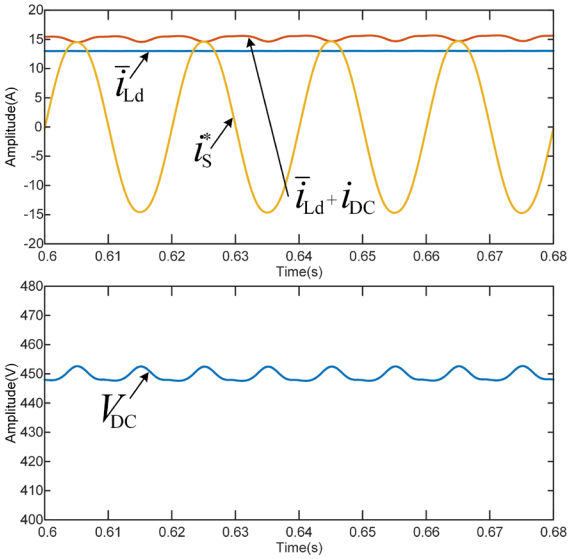

Figure 10 $\bar{\imath}_{Ld}$, $\bar{\imath}_{Ld} + i_{DC}$, i_s^* and V_{DC}: After compensation

Figure 11(a) illustrates the control performance of the proposed active filter circuit. The supply current effectively tracks the reference current, reducing the total harmonic distortion (THDi) of the supply current from 58.84% to 2.21%, specifically with a nonlinear load. **Figure 11(b)** compares the load current (i_L), supply current (i_s), compensation current (i_{sh}), and the DC bus voltage (V_{DC}). It is noticeable that the supply current closely approximates a sinusoidal waveform.

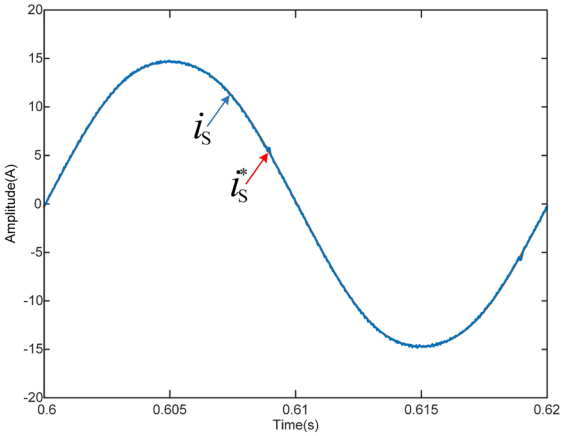

(a) i_s^*, i_s: After compensation

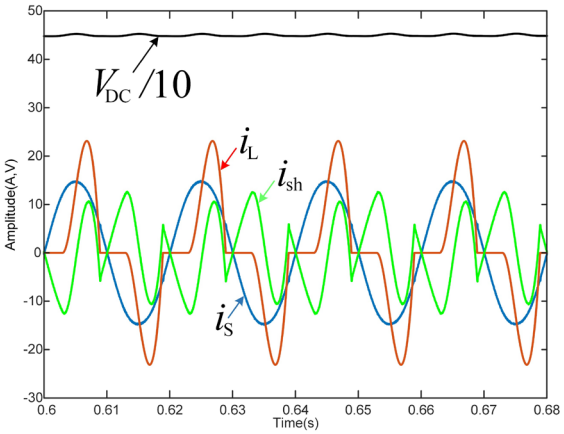

(b) V_{DC}, i_s, $i_L$and i_{sh}: After compensation

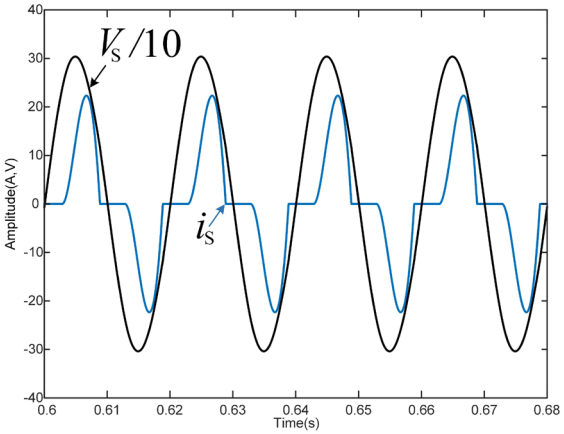

(c) V_s, i_s: Before compensation

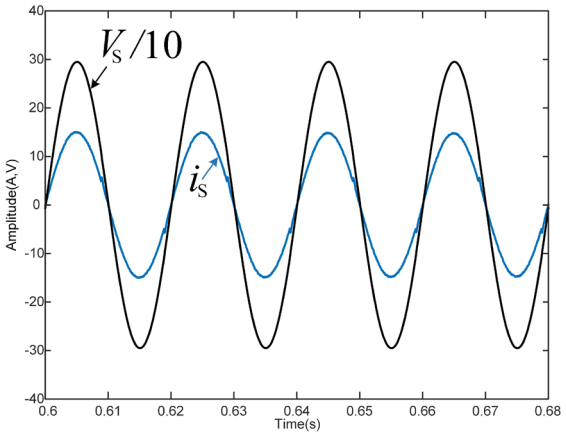

(d) V_s, i_s: After compensation

Figure 11 Performance of single-phase SAF: Before & After compensation (Simulation results)

Figure 12 shows the simulation of the single-phase shunt active power filter (SAF) circuit with indirect current control, where both a linear load and a nonlinear load are connected to the system to evaluate the performance of the proposed circuit. **Figure 13** illustrates the system's response during simulation when a linear load is added at time t = 1.2 s. It can be observed that the current waveform of i_L increases, with its shape changing. This also causes an increase in the supply current i_s due to the added load. As shown in **Figure 14**, the DC bus voltage drops momentarily at t = 1.2 s. However, the system still manages to converge to the reference signal V_{DC}^* at 450 volts within approximately 1 second. Additionally, the compensating current control loop i_s remains controllable, closely tracking the reference current i_s^*, as shown in **Figure 15(a)**, reducing the total harmonic distortion of current (THDi) from 43.14% to 1.36%.

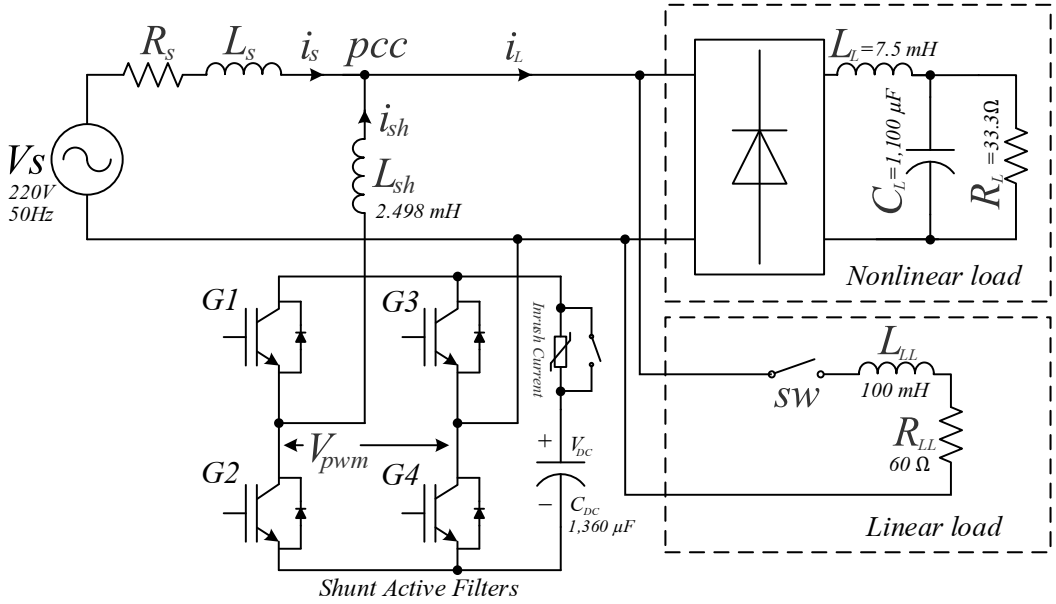

Figure 12 The structure of the single-phase SAF circuit simulated with a linear load

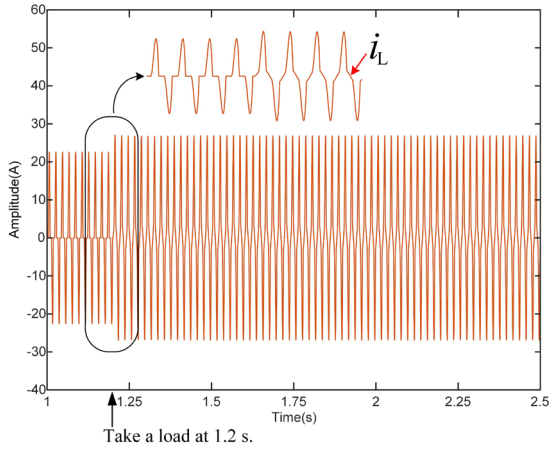

Figure 13 The waveform of i_L when a linear load is added at time t = 1.2s.

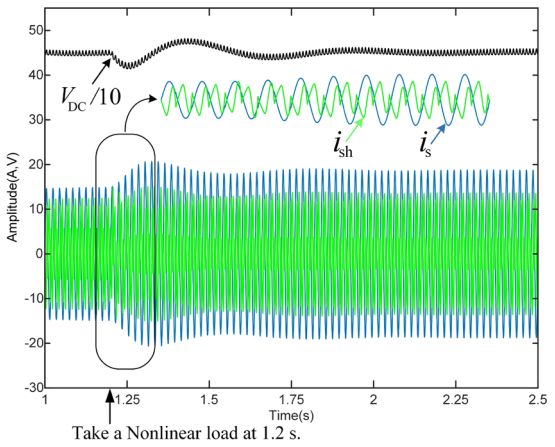

Figure 14 The waveform of i_s, i_{sh} and V_{DC} when a linear load is added at time t = 1.2s.

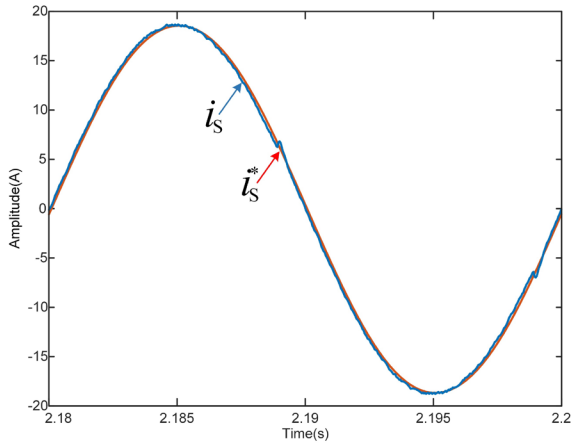

(a) i_s^*, i_s: After compensation (Add a linear load)

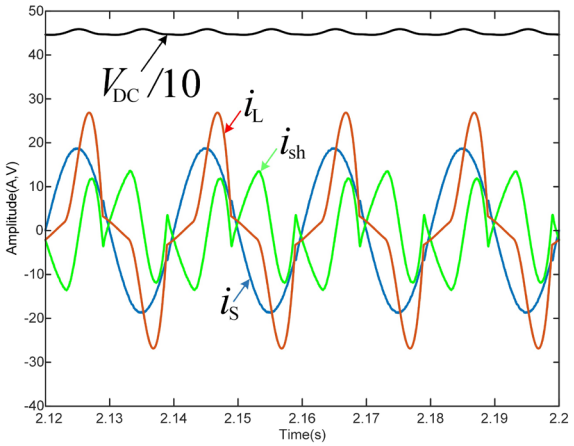

(b) V_{DC}, i_s, i_L and i_{sh}: After compensation (Add a linear load)

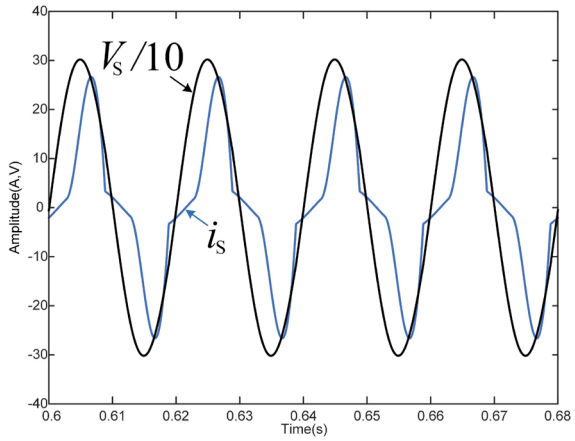

(c) V_s, i_s: Before compensation (Add a linear load)

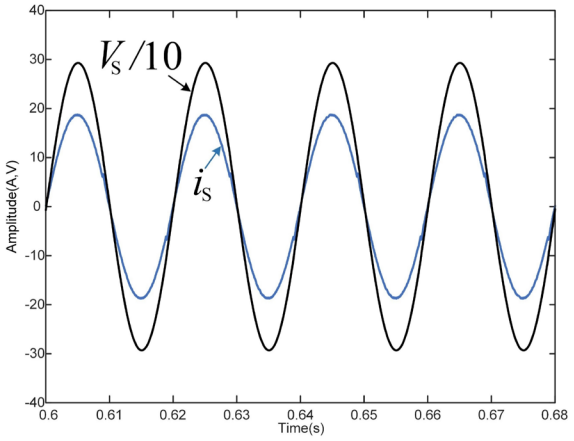

(d). V_s, i_s: After compensation (Add a linear load)

Figure 15 Performance of single-phase SAF with the addition of a linear load: Before & After compensation (Simulation results)

4.2 Experimental Results

The experiments were carried out utilizing dSPACE and Control Desk within MATLAB/ SIMULINK. The obtained experimental results are very close to the assumptions made in every aspect, as depicted in the accompanying figure. The actual results from the experiments strongly support the parameter values used in the simulation model, thus validating the proposed system hypothesis. The experimental results for the input signals to the system when it is not yet operational, and the input signals obtained from the measurement circuits, are sent to the ADC channels of the dSPACE Interfacing Card. These measured signals include the supply voltage (V_s), the DC bus voltage (V_{DC}) obtained from the voltage measurement circuit, as well as the supply current (i_s), load current (i_L), and active inductor current (i_{sh}) from the current measurement circuit, as shown in **Figure 16**.

The experimental results for load current detection to generate the reference signal for the single-phase shunt active power filter with indirect current control, as described in sections 3.1 and 4.1, detail the design of the load current detector to generate the reference signal (i_s^*) for the single-phase shunt active power filter controlled in the d-q reference frame. This was simulated using MATLAB/SIMULINK (SimPower-Systems). This section presents the experimental results obtained from actual experiments to indicate that the results are consistent with the previously designed simulation results, as shown in **Figures 17–22**. **Figures 23–24** illustrate the comparison results of a chart showing the total harmonic distortion (THD) of the supply current before and after harmonic current compensation, respectively. **Figure 25** shows the hardware of the single-phase SAF used in this experiment.

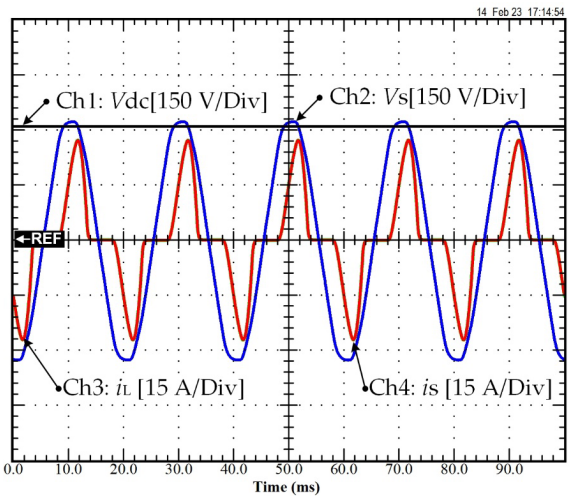

Figure 16 V_s, i_s, i_L and V_{DC}: Before compensation

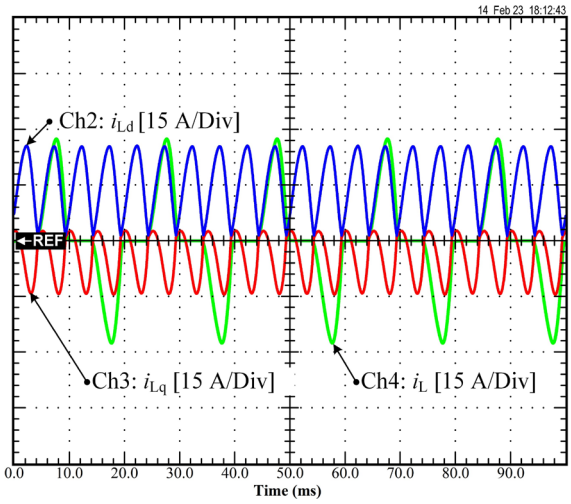

Figure 19 i_{Ld}, i_{Lq} and i_L

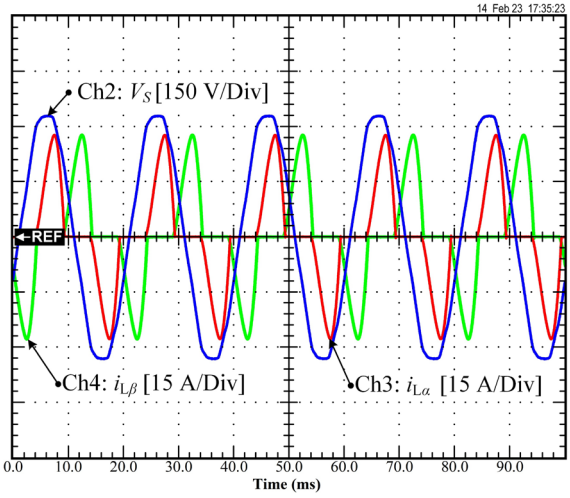

Figure 17 V_s, $i_{L\alpha}$ and $i_{L\beta}$

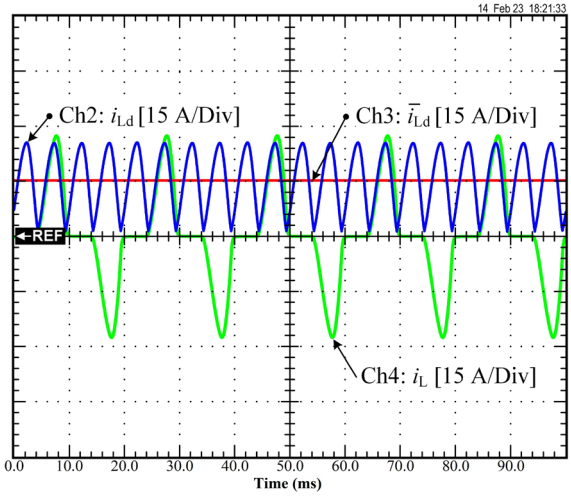

Figure 20 i_{Ld}, $\bar{i}_{Ld}$, and i_L

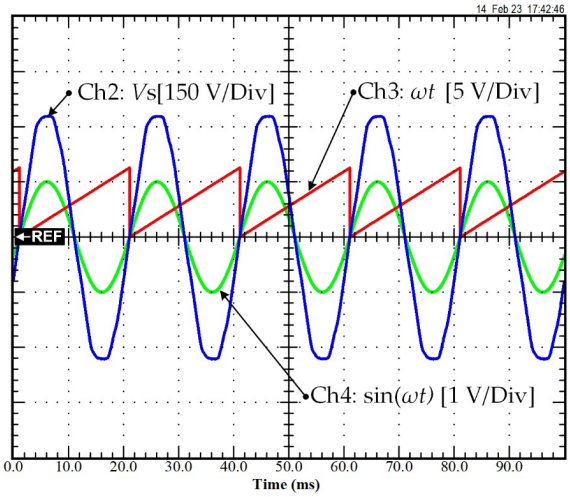

Figure 18 ωt and $sin\ \omega\ t$ compared to the voltage waveform V_s

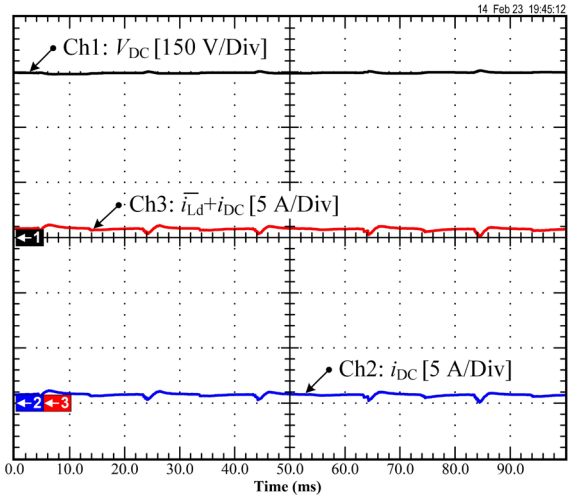

Figure 21 V_{DC}, i_{DC} and $\bar{i}_{Ld} + i_{DC}$

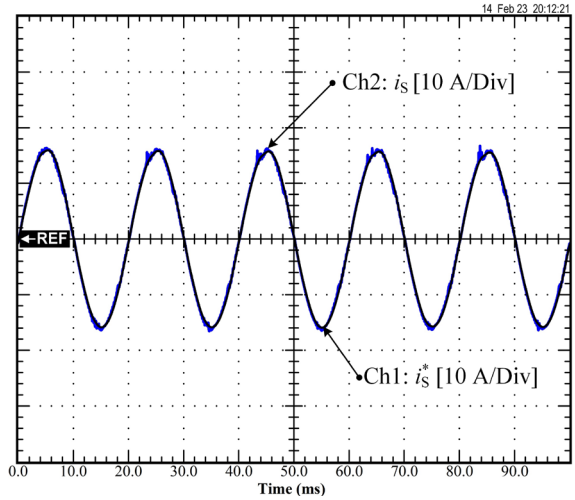

(a). i_s^*, i_s

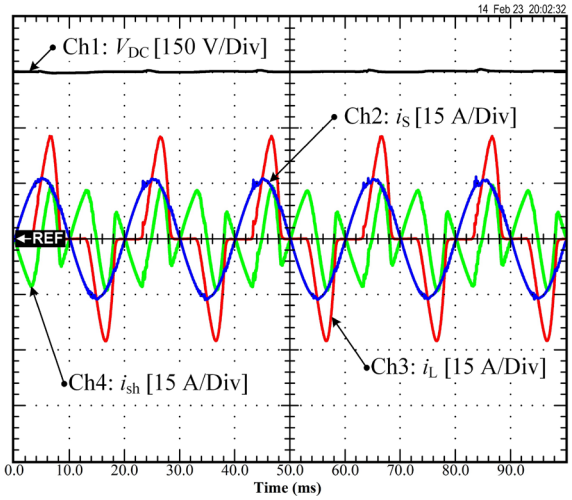

(b). V_{DC}, i_s, i_L and i_{sh}: After compensation

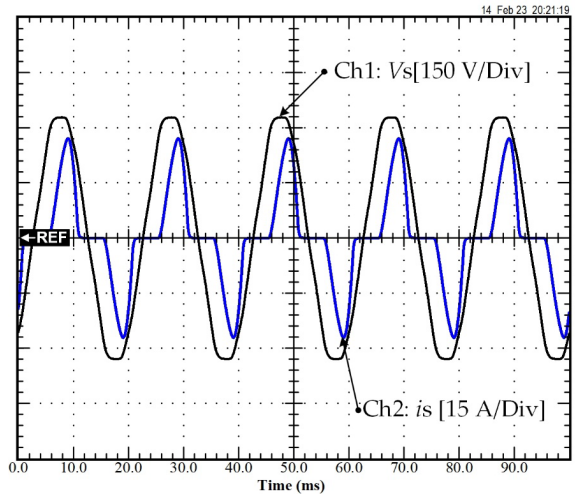

(c). V_s, i_s: Before compensation

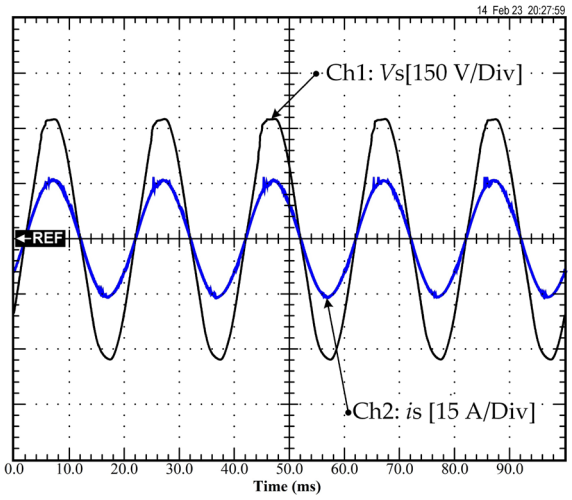

(d). V_s, i_s: After compensation

Figure 22 Performance of single-phase SAF: Before & After compensation (Experimental results)

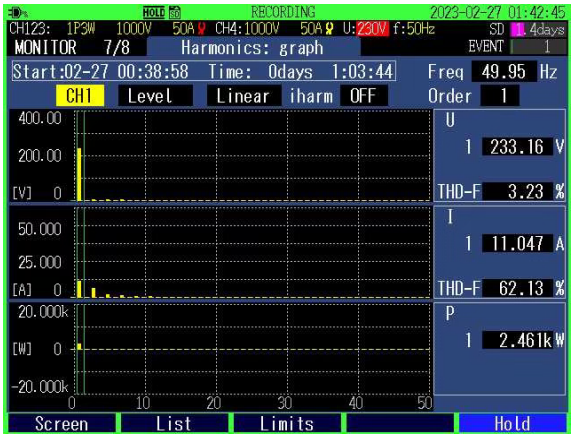

Figure 23 Chart illustrating the total harmonic distortion (THD) of a supply current. Without single-phase SAF

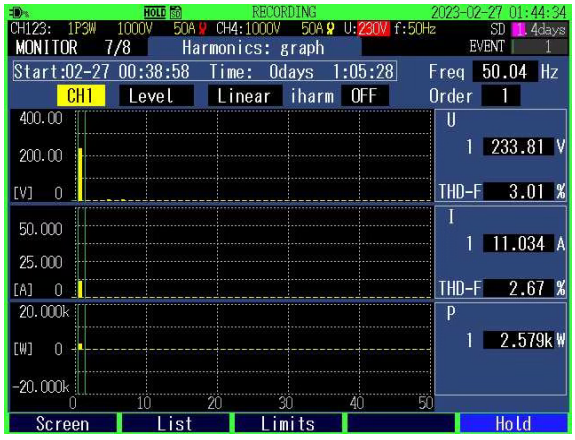

Figure 24 Chart illustrating the total harmonic distortion (THD) of a supply current. With single-phase SAF

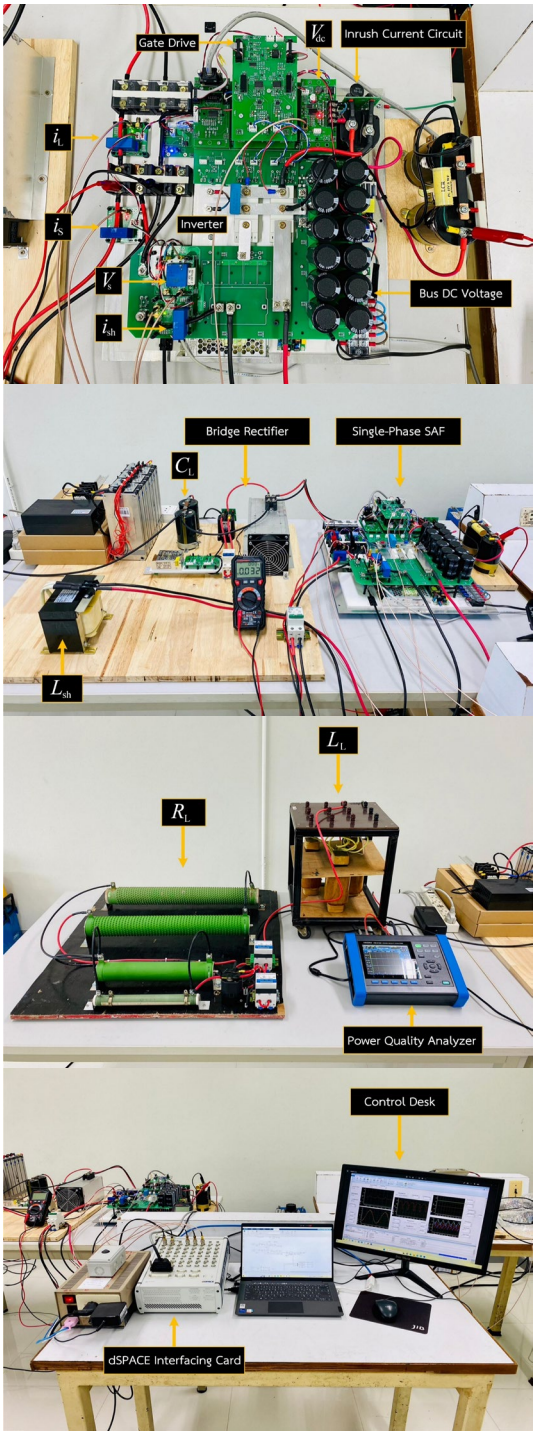

Figure 25 Hardware of a Single-Phase SAF

5. Conclusion

This research presents a circuit set designed to address the issue of harmonic currents caused by non-linear loads using a single-phase shunt active filter. The filter employs indirect current control, allowing the use of a simple PI controller, which is widely utilized in the industry. The controller gains are determined and selected based on appropriate values for damping and natural frequency control. The reference current signal is generated using the single-phase synchronous d-q reference frame method. Simulations and experiments demonstrate the system's efficiency in mitigating harmonic currents, meeting the IEEE Std 519-2022 standards. The results showcase excellent control of the supply current in steady-state conditions. In the simulation, the total harmonic distortion (THD) of the supply current is reduced from 58.84% to 2.21%, and in the experimental setup, it is reduced from 62.13% to 2.67%, as shown in **Table 2**.

Table 1 Specification and Parameters of The Single-Phase Shunt Active Filter

AC supply voltage	230 V, 50 Hz
Nonlinear load (Bridge Rectifier) Inductor (L_L), Capacitor (C_L), Resister (R_L)	 1,600 V, 100 A 7.5 mH, 1,100 μF, 33.3 Ω
Active Filter impedance (L_{sh}, R_{sh})	2.498 mH, 0.124 Ω
DC voltage reference (V_{DC}^{*})	450 V
DC-link capacitor (C_{DC})	1,360 μF, 900 V
Inverter Rate	10 kW
Switching frequency (f_s)	25 kHz
Sampling time of simulation	0.4 μs
Sampling time of experiment on dSPACE	0.4 μs
Gain of K_{pi}	0.1118
Gain of K_{ii}	500
Gain of K_{pv}	0.0152
Gain of K_{iv}	0.6805
IGBTs	1,200 V, 100 A

Table 2 Comparison of the Total Harmonic Current Distortion (THDi) Before and After Using a Single-Phase Shunt Active Filter

	Before (THDi)	After (THDi)
Simulation	58.84%	2.21%
Experimental	62.13%	2.67%

6. Acknowledgements

The research team would like to express gratitude to Thailand Science Research and Innovation (TSRI) for providing funding support for this research project. We also extend our thanks to the Faculty of Industry and Technology and the Institute of Research and Development at Rajamangala University of Technology Rattanakosin (RMUTR) for facilitating laboratory facilities, as well as for monitoring progress and handling document deliveries related to the research project.

7. References

[1] V. E. Wagner, J. C. Balda, D. C. Griffith, A. McEachern, T. M. Barnes, D. P. Hartmann, D. J. Phileggi, A. E. Emannuel, W. F. Horton, W. E.

Reid *et al.*, "Effects of harmonics on equipment," *IEEE Transactions on Power Delivery*, vol. 8, no. 2, pp. 672–680, 1993, doi: 10.1109/61.216874.

[2] B. Singh, K. Al-Haddad and A. Chandra, "A review of active filters for power quality improvement," *IEEE Transactions on Industrial Electronics*, vol. 46, no. 5, pp. 960–971, 1999, doi: 10.1109/41.793345.

[3] El-Habrouk, M., Darwish, M.K. and Mehta, P., "Active Power Filters: a Review," *IEE Proceedings-Electric Power Applications*, vol. 147, no. 5, pp. 403–413, 2000, doi: 10.1049/ip-epa:20000522.

[4] D. Çelik, H. Ahmed and M. E. Meral, "Kalman Filter-Based Super-Twisting Sliding Mode Control of Shunt Active Power Filter for Electric Vehicle Charging Station Applications," *IEEE Transactions on Power Delivery*, vol. 38, no. 2, pp. 1097–1107, 2023, doi: 10.1109/TPWRD.2022.3206267.

[5] A. M. Massoud, S. J. Finney and B. W. Williams, "Review of harmonic current extraction techniques for an active power filter," in *2004 11th International Conference on Harmonics and Quality of Power (IEEE Cat. No.04EX951)*, Lake Placid, NY, USA, Sep. 12–15, 2004, pp. 154–159, doi: 10.1109/ICHQP.2004.1409345.

[6] V. Khadkikar, M. Singh, A. Chandra and B. Singh, "Implementation of single-phase synchronous d-q reference frame controller for shunt active filter under distorted voltage condition," in *2010 Joint International Conference on Power Electronics, Drives and Energy Systems & 2010 Power India*, New Delhi, India, Dec. 20–23, 2010, pp. 1–6, doi: 10.1109/PEDES.2010.5712526.

[7] M. Miletić, K. R. Raguž, V. Zeleničić, I. Erceg and D. Sumina, "Development of Single-Phase Shunt Active Power Filter for Reduction of Current Harmonics in Data Center Power System," in *2023 11th International Conference on Smart Grid (icSmartGrid)*, Paris, France, Jun. 4–7, 2023, pp. 1–7, doi: 10.1109/icSmartGrid58556.2023.10170839.

[8] T. Narongrit, P. Santiprapan and S. Janpong, "A Synchronous Detection with Fourier Analysis for Single-Phase Shunt Active Power Filters," in *2018 5th International Conference on Electric Power and Energy Conversion Systems (EPECS)*, Kitakyushu, Japan, Apr. 23–25, 2018, pp. 1–6, doi: 10.1109/EPECS.2018.8443528

[9] M. H. Alaee, S. A. Taher and Z. Dehghani Arani, "Improved performance of single-phase shunt active power filter by using conservative power theory and model predictive control," in *2018 9th Annual Power Electronics, Drives Systems and Technologies Conference (PEDSTC)*, Tehran, Iran, Feb. 13–15, 2018, pp. 163–168, doi: 10.1109/PEDSTC.2018.8343790

[10] A. Mohamed, S. Zaid and O. Mahgoub. "Improved active power filter performance based on an indirect current control technique," *Journal of power electronics (JPE)*, vol. 11, no. 6, pp.931–937, 2011, doi: https://doi.org/10.6113/JPE.2011.11.6.931.

[11] Q. -N. Trinh and H. -H. Lee, "An Advanced Current Control Strategy for Three-Phase Shunt Active Power Filters," *IEEE Transactions on Industrial Electronics*, vol. 60, no. 12, pp. 5400–5410, 2013, doi: 10.1109/TIE.2012.2229677.

[12] H. Usman, H. Hizam and M. A. Mohd Radzi, "Simulation of single-phase shunt active power filter with fuzzy logic controller for power quality improvement," in *2013 IEEE Conference on Clean Energy and Technology (CEAT)*, Langkawi, Malaysia, Nov. 18–20, 2013, pp. 353–357, doi: 10.1109/CEAT.2013.6775655.

[13] A. Zafari, M. Mehrasa, M. Sharifzadeh, S. Bacha, K. Al-Haddad and N. Hosseinzadeh, "A Novel Reference Current Detection Algorithm (RCDA) in 9-Level PEC Converter-based Shunt Active Power Filter," in *2021 22nd IEEE International Conference on Industrial Technology (ICIT)*, Valencia, Spain, Mar. 10–12, 2021, pp. 272–277, doi: 10.1109/ICIT46573.2021.9453502.

[14] A. R. Dash and A. K. Panda, "Experimental validation of a shunt active filter based on cascaded multilevel inverter with single excited DC source," in *2018 International Conference on Power, Instrumentation, Control and Computing (PICC)*, Thrissur, India, Jan. 18–20, 2018, pp. 1–6, doi: 10.1109/PICC.2018.8384799.

[15] S. Boonto and W. Lenwari, "Two-degree-of-freedom $\mathscr{H}^{\infty}$ control design for harmonic current control of shunt active filters," in *2012 IEEE 15th International Conference on Harmonics and Quality of Power*, Hong Kong, China, Jun. 17–20, 2012, pp. 887–891, doi: 10.1109/ICHQP.2012.6381220.

[16] K. Nishida, M. Rukonuzzman and M. Nakaoka, "Advanced Current Control Implementation with Robust Deadbeat Algorithm for Shunt Single-Phase Voltage-Source Type Active Power Filter," *IEE Proceedings-Electric Power Applications*, vol. 151, no. 3, pp. 283–288, 2004, doi: 10.1049/ip-epa:20040317.

[17] W. Lenwari, "Optimized design of modified proportional-resonant controller for current control of active filters," in *2013 IEEE International Conference on Industrial Technology (ICIT)*, Cape Town, South Africa, Feb. 25–28, 2013, pp. 894–899, doi: 10.1109/ICIT.2013.6505789.

[18] S. Rahmani, K. Al-Haddad and F. Fnaiech, "Reduced switch number single-phase shunt active power filter using an indirect current control technique," in *IEEE International Conference on Industrial Technology, 2003*, Maribor, Slovenia, Dec. 10–12, 2003, pp. 1107–1112, doi: 10.1109/ICIT.2003.1290818.

[19] H. Yi, F. Zhuo, Y. Zhang, Y. Li, W. Zhan, W. Chen, J. Liu *et al.*, "A Source-Current-Detected Shunt Active Power Filter Control Scheme Based on Vector Resonant Controller," *IEEE Transactions on*

Industry Applications, vol. 50, no. 3, pp. 1953–1965, 2014, doi: 10.1109/TIA.2013.2289956.

[20] A. Bouhouta, S. Moulahoum, N. Kabache and I. Colak, "Experimental Investigation of Fuzzy Logic Controller Based Indirect Current Control Algorithm for Shunt Active Power Filter," in *2019 8th International Conference on Renewable Energy Research and Applications (ICRERA)*, Brasov, Romania, Nov. 3–6, 2019, pp. 309–314, doi: 10.1109/ICRERA47325.2019.8997115.

[21] A. Bouhouta, S. Moulahoum, N. Kabache and A. Benyamina, "Design and Real Time Implementation of Three Phase Shunt Active Power Filter Using Indirect Current Control Technique," in *2019 International Conference on Advanced Electrical Engineering (ICAEE)*, Algiers, Algeria, Nov. 19–21, 2019, pp. 1–6, doi: 10.1109/ICAEE47123.2019.9015096.

[22] K. Yodmanee and W. Lenwari, "PI controller optimization for indirect current control for single-phase shunt active filter," *Ladkrabang Engineering Journal*, vol. 33, no. 1, pp.42–47, 2016.

[23] S. Waosungnern, T. Narongrit and K. Areerak, "Design of a Shunt Active Power Filter for Single-Phase Power Systems," *TNI Journal of Engineering and Technology*, vol. 9, no. 1, pp.27–36, 2021.

[24] S. Sriprang, N. Poonnoy, D. Guilbert, B. Nahid-Mobarakeh, N. Takorabet, N. Bizon and P. Thounthong, "Design, Modeling, and Differential Flatness Based Control of Permanent Magnet-Assisted Synchronous Reluctance Motor for e-Vehicle Applications," *Sustainability*, vol. 13, no. 17, 2021, Art. no. 9502, doi: 10.3390/su13179502.